XLP: A Cross-Layer Protocol for Efficient Communication in Wireless Sensor Networks

Mehmet C. Vuran, *Member*, *IEEE*, and Ian F. Akyildiz, *Fellow*, *IEEE*

Abstract—Severe energy constraints of battery-powered sensor nodes necessitate energy-efficient communication in Wireless Sensor Networks (WSNs). However, the vast majority of the existing solutions are based on the classical layered protocol approach, which leads to significant overhead. It is much more efficient to have a unified scheme, which blends common protocol layer functionalities into a cross-layer module. In this paper, a cross-layer protocol (XLP) is introduced, which achieves congestion control, routing, and medium access control in a cross-layer fashion. The design principle of XLP is based on the cross-layer concept of *initiative determination*, which enables receiver-based contention, initiative-based forwarding, local congestion control, and distributed duty cycle operation to realize efficient and reliable communication in WSNs. The initiative determination requires simple comparisons against thresholds, and thus, is very simple to implement, even on computationally constrained devices. To the best of our knowledge, XLP is the first protocol that integrates functionalities of all layers from PHY to transport into a cross-layer protocol. A cross-layer analytical framework is developed to investigate the performance of the XLP. Moreover, in a cross-layer simulation platform, the state-of-the-art layered and cross-layer protocols have been implemented along with XLP for performance evaluations. XLP significantly improves the communication performance and outperforms the traditional layered protocol architectures in terms of both network performance and implementation complexity.

Index Terms—Cross-layer protocol, congestion control, routing, medium access control, wireless sensor networks.

1 Introduction

Wireless sensor networks (WSNs) are event-based systems that exploit the collective effort of densely deployed sensor nodes and continuously observe a certain physical phenomenon. The main goal is to reliably detect/estimate event features from the collective information provided by sensor nodes respecting their limited energy, storage, and processing capabilities. To this end, there have been a significant number of research efforts that aim to develop collaborative networking protocols to achieve communication with maximum energy efficiency.

The majority of the communication protocols are individually developed and optimized for different networking layers, i.e., transport, network, medium access control (MAC), and physical layers. While these protocols achieve very high performance in terms of the metrics related to each of these individual layers, they are not jointly designed and optimized to maximize the overall network performance while minimizing the energy expenditure. Considering the scarce energy and processing resources of WSNs, joint design of networking layers, i.e., *cross-layer design*, stands as the most promising alternative that has gained interest recently.

Recent results [11], [13] reveal that cross-layer integration and design techniques result in significant improvement in terms of energy efficiency in WSNs. These results have, recently, led to several solutions on the cross-layer interaction and design. A detailed discussion of these solutions can be found in [22]. However, as discussed in Section 2, these studies either provide analytical results without any communication protocol design or perform cross-layer design within a limited scope, e.g., routing and MAC layers.

Clearly, there is still much to be gained by rethinking the functionalities of protocol layers in a unified way so as to provide a single communication module for efficient communication in WSNs. To this end, this paper introduces a novel concept, i.e., *initiative determination*, and illustrates how certain traditional networking functionalities can be jointly designed based on this concept to implement a cross-layer operation of medium access, distributed routing, and local congestion control functionalities. The *initiative determination* procedure is used for each node to decide on participating in communication based on its current state related to link quality, location, current traffic load, buffer level, and remaining energy level. These fundamental operation states are incorporated into a unified decision incentive to define a node's level of willingness in participating in the communication. Accordingly, a cross-layer protocol (XLP) is developed to achieve efficient and reliable event communication in WSNs with minimum energy expenditure.[1] In a cross-layer simulation platform, the state-of-the-art layered and cross-layer protocol configurations have been implemented along with XLP to provide a complete performance evaluation. Analytical performance evaluation and simulation experiment results show that XLP significantly improves

- *M.C. Vuran is with the Cyber-Physical Networking Laboratory, Department of Computer Science and Engineering, University of Nebraska—Lincoln, 109 Schorr Center, Lincoln, NE 68588.*
  E-mail: mcvuran@cse.unl.edu.
- *I.F. Akyildiz is with the Broadband Wireless Networking Laboratory, School of Electrical and Computer Engineering, Georgia Institute of Technology, Centergy One, Room 5170, Atlanta, GA 30332.*
  E-mail: ian@ece.gatech.edu.

Manuscript received 13 Oct. 2007; revised 22 Oct. 2008; accepted 17 Mar. 2010; published online 28 June 2010.
For information on obtaining reprints of this article, please send e-mail to: tmc@computer.org, and reference IEEECS Log Number TMC-2007-10-0312.
Digital Object Identifier no. 10.1109/TMC.2010.125.

[1] A preliminary version of this work appeared in [2].

the communication performance and outperforms the traditional layered and recent cross-layer protocol architectures in terms of both network performance and implementation complexity. These results highlight the advantages of the initiative concept, which is a novel perspective for networking in WSNs.

The remainder of the paper is organized as follows: In Section 2, we provide a review of existing work on cross-layer design in WSNs. The XLP basics, overview, and protocol description are introduced in Section 3 as well as the theoretical analysis framework. In Section 4, we provide performance evaluations of the XLP solution and provide a comparative analysis with five layered suites. Finally, the paper is concluded in Section 5.

2 Related Work

Recently, receiver-based contention techniques have been adopted in several cross-layer MAC and routing protocols [22] (see references therein). However, most of these protocols focus on the interaction between MAC and routing layers and omit the transport layer and physical layer issues. In [25], a receiver-based routing protocol is proposed, where the performance of the protocol is analyzed based on a simple channel model and lossless links. Moreover, the latency performance of the protocol is presented based on different delay functions and collision rates. Also, the effects of the physical layer are not considered in the protocol operation.

In [2], we have developed the cross-layer protocol (XLP), which integrates physical, MAC, routing, as well as transport layer functionalities into a unified communication framework. In this work, we extend this protocol to distributively account for the local minima experienced by geographical routing protocols, provide an analytical analysis of the XLP protocol, and perform extensive comparative evaluations including state-of-the-art layered and cross-layer protocols.

The adaptive load balanced algorithm (ALBA-R) is described in [3], where, in addition to the location of the nodes, the traffic load on each node is considered for route establishment. More specifically, each potential node computes two values: geographic priority index (GPI) and queue priority index (QPI), which indicate the progress of the node towards the destination and its traffic load, respectively. Accordingly, if a node has a packet to send, it sends several RTS packets to scan QPI and GPI values of its neighbors. Each neighbor responds to this packet by CTS packets if their values match the requested values. The source node then selects one of the neighbors if the requested value is found. Moreover, ALBA-R aims to avoid local minima in routing through a coloring scheme called Rainbow. Based on its previous success in finding relays, each node assigns itself a different color, which is used to participate in communication. While ALBA-R employs a cross-layer MAC/routing technique, the route selection is performed at the sender node, which incurs high overhead due to the QPI and GPI scanning. Moreover, the transport layer issues such as congestion control are not completely addressed in ALBA-R as we will discuss in Section 4.

In [9], an integrated MAC/routing (MACRO) protocol is developed, where the next hops are selected according to a weighted progress factor, which considers the progress toward destination per transmitted power. MACRO also employs the receiver-based contention scheme but considers only energy efficiency and geographical locations for communication. The convergent MAC (CMAC) protocol is developed in [19], where next hop nodes are selected according to a normalized latency metric. The CTS replies are prioritized according to this metric and the routes are selected based on this prioritization mechanism. In [23], a routing protocol is proposed, where a weighted cost function including position cost, queuing cost, and remaining energy cost is used for relay selection. The position cost is associated with the angular offset of the potential relay node from the base station as seen by the transmitting node.

While there exist several cross-layer protocols that exploit the receiver-based contention and geographical routing principles, these solutions are limited to MAC and routing cross-layer operation. However, network congestion and link reliability that are related to transport and physical layer functionalities are yet to be considered in a unified cross-layer protocol.

In [5] and [6], a cross-layer optimization solution for power control at the physical layer and congestion control at the transport layer is considered. Moreover, a cross-layer analysis of the impact of physical layer constraints on link-level and network-level performance of CDMA sensor networks is presented in [8]. This work underlines important trade offs between topology control and receiver design principles. However, these studies apply only to CDMA-based wireless multihop networks which may not apply to WSNs where CDMA technology may not be the most efficient scheme.

In [24], new forwarding strategies for geographic routing are proposed based on the analytical work in [33]. Expressions for the optimal forwarding distance for networks with and without ARQ are also provided. However, the forwarding protocol does not consider the impact of medium access and results in a high overhead. Moreover, the analysis for the distribution of optimal hop distance is based on a linear network structure, which may not be practical for WSNs, where a two-dimensional terrain exists.

In [7], a joint routing, MAC, and link layer optimization framework is proposed. Although the optimization framework is insightful, a communication protocol for practical implementation is not developed. Moreover, the transport layer issues such as congestion and flow control are not considered. Furthermore, in [17] and [18], a thorough investigation of optimization techniques for cross-layer design in wireless networks are performed. It has been stated that scheduling constitutes the bottleneck in optimization due to the nonconvex nature of the scheduling problem. Consequently, in [18], a distributed cross-layer congestion control and scheduling algorithm is developed. However, the provided solution focuses only on two layers for cross-layer design including transport and link layers.

These studies either provide analytical results without any communication protocol design, or perform cross-layer design within limited scope, e.g., only routing and MAC. In this paper, we argue that a new networking paradigm is required to design a cross-layer protocol that addresses medium access, routing, and congestion issues in WSNs.

3 XLP: Cross-Layer Protocol for WSNs

The design principle of XLP is a unified cross layering such that both the information and the functionalities of three fundamental communication paradigm (medium access, routing, and congestion control) are considered in a single protocol operation. Consequently, XLP incorporates the required functionalities by considering the channel effects.[2] The details of these functionalities are explained in the following sections. Before explaining the specifics of the XLP operation, we first introduce the *initiative determination* concept, which constitutes the core of the XLP.

3.1 Initiative Determination

The *initiative determination* concept coupled with the receiver-based contention mechanism provides freedom to each node participating in communication. In WSNs, the major goal of a communication suite is to successfully transport event information by constructing (possibly) multihop paths to the sink. To this end, the cross-layer initiative determination concept constitutes the core of the XLP and implicitly incorporates the intrinsic communication functionalities required for successful communication in WSNs.

Consider a node, i, which initiates transmission by informing its neighbors that it has a packet to send. This is achieved by broadcasting a request to send (RTS) packet. Upon receiving this packet, each neighbor of node i decides to participate in the communication or not. This decision is made through the *initiative determination* based on the current state of the node. The initiative determination is a binary operation where a node decides to participate in communication if its initiative is 1. Denoting the initiative as $\mathcal{I}$, it is determined as follows:

$$\mathcal{I} = \begin{cases} 1, & \text{if} \begin{cases} \xi_{RTS} \geq \xi_{Th} \\ \lambda_{relay} \leq \lambda_{relay}^{Th} \\ \beta \leq \beta^{max} \\ E_{rem} \geq E_{rem}^{min}, \end{cases} \\ 0, & \text{otherwise.} \end{cases} \tag{1}$$

The initiative is set to 1 if all four conditions in (1) are satisfied, where each condition constitutes a certain communication functionality in XLP. The first condition, i.e., $\xi_{RTS} \geq \xi_{Th}$, ensures reliable links to be constructed for communication based on the current channel conditions. For this purpose, it is required that the received signal-to-noise ratio (SNR) of an RTS packet, ξ_{RTS}, is above some threshold ξ_{Th} for a node to participate in communication. The effect of this threshold on routing and energy consumption performance will be analyzed and the most efficient value of this threshold will be chosen in Section 3. The second, i.e., $\lambda_{relay} \leq \lambda_{relay}^{Th}$, and the third, i.e., $\beta \leq \beta^{max}$, conditions are used for local congestion control in XLP. As will be explained in Section 3.6, the second condition prevents congestion by limiting the traffic a node can relay. More specifically, a node participates in the communication if its relay input rate, λ_{relay}, is below some threshold λ_{relay}^{Th}. The third condition ensures that the buffer occupancy level of a node, β, does not exceed a specific threshold, β^{max}, so that the node does not experience buffer overflow and the congestion is prevented. The last condition, i.e., $E_{rem} \geq E_{rem}^{min}$, ensures that the remaining energy of a node E_{rem} stays above a minimum value, E_{rem}^{min}. This constraint helps preserve uniform distribution of energy consumption throughout the network.

The cross-layer functionalities of XLP lie in these constraints that define the *initiative* of a node to participate in communication. Using the initiative concept, XLP performs receiver-based contention, initiative-based forwarding, local congestion control, hop-by-hop reliability, and distributed operation. The details of XLP operation are explained next. More specifically, we first define the basic parameters and the network model considered for the operation of XLP in Section 3.2. For a successful communication, a node first initiates transmission using a broadcast message as explained in Section 3.3. Then, the neighbors that receive this message perform initiative determination. The neighbors that decide to participate in communication perform receiver-based contention or angle-based routing as described in Section 3.4 and Section 3.5, respectively. Moreover, the local congestion control component ensures energy-efficient as well as reliable communication by two-step congestion control as explained in Section 3.6. Finally, based on this protocol operation description, the operation of XLP is analytically investigated in Section 3.7.

3.2 Basics, Definitions, and Network Model

We assume the following network model for the operation of XLP: Each node performs a distributed duty cycle operation such that the transceiver circuit of the node is *on* for a certain fraction of the time and is switched *off* for the remaining fraction of the time during which the sensors can still sample data. The on-off periods are managed through a *duty cycle parameter*, δ, which defines the fraction of the time a node is active. More specifically, each node is implemented with a sleep frame with length T_S sec. A node is active for $\delta \times T_S$ sec and is asleep state for $(1 - \delta) \times T_S$ sec. Note that the start and end times of each node's sleep cycle are not synchronized. Consequently, a distributed duty cycle operation is employed. Furthermore, we assume that each node is aware of its location. This assumption is motivated by the fact that WSN applications inherently require location information to associate the observed information by each node to a physical location. Hence, each node is required to be aware of its location, which can be provided through either an onboard GPS or a localization algorithm [20]. Thus, it is only natural to leverage this information for communication. The network model is also geared toward event-based information flow, where nodes send information to a single stationary sink if an event occurs in their vicinity. The area that an event occurs is denoted by the event area and the nodes in this area generate event information. Based on this network model, the protocol operation details are explained in the following sections according to Fig. 1.

[2] Note that the sensor nodes equipped with XLP will still have RF transceivers, which have all necessary physical-layer functionalities, e.g., modulation/demodulation, channel coding, and RF power control, specified according to the specific deployment and application requirements.

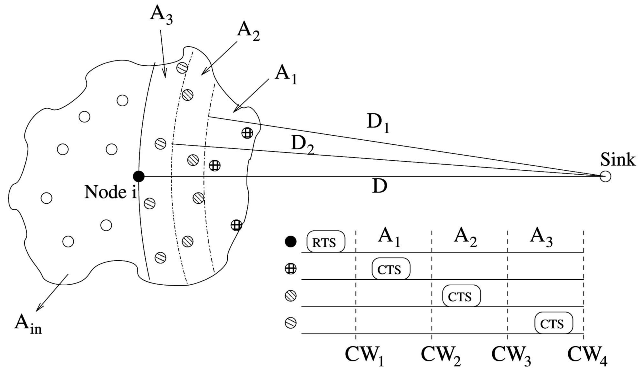

Fig. 1. Priority regions and the prioritization mechanism.

3.3 Transmission Initiation

When a node i has a packet to transmit, it first listens to the channel for a specific period of time. If the channel is occupied, the node performs backoff based on its contention window size, CW_{RTS}. When the channel is idle, the node broadcasts an RTS packet, which contains the location information of itself and the sink. This packet also serves as a link quality indicator and helps the neighbors to perform receiver contention, which is explained in Section 3.4. When a neighbor of node i receives an RTS packet, it first checks the source and destination locations. We refer to the region where the neighbors of a node that are closer to the sink reside as the *feasible region* and the remaining neighborhood as the *infeasible region*. A node which receives a packet first checks if it is inside the feasible region. To save energy, nodes inside the infeasible region switch to sleep for the duration of the communication. The nodes inside the feasible region perform initiative determination as explained in Section 3. If a node decides to participate in communication, it performs *receiver contention* as explained next.

3.4 Receiver Contention

The receiver contention operation of XLP leverages the initiative determination concept with the receiver-based routing approach [2]. After an RTS packet is received, if a node has an initiative to participate in the communication, i.e., $\mathcal{I} = 1$, it performs receiver contention to forward the packet. The receiver contention is based on the routing level of each node, which is determined based on the progress a packet would make if the node forwards the packet. The feasible region is divided into N_p priority regions, i.e., A_i, $i = 1, ..., N_p$. Nodes with longer progress have higher priority over other nodes. According to the location information, each node determines its priority region and performs contention for medium access as explained next.

Each priority region, A_i, corresponds to a backoff window size, CW_i. Based on its location, a node backs off for $\sum_{j=1}^{i-1} CW_j + cw_i$, where cw_i is randomly chosen such that $cw_i \in [0, CW_{max}]$, where $CW_{max} = CW_i - CW_{i-1}$, $\forall i$. This backoff scheme helps differentiate nodes of different progress into different prioritization groups. Only nodes inside the same group contend with each other. The winner of the contention sends a CTS packet to node i indicating that it will forward the packet. On the other hand, if during backoff, a potential receiver k receives a CTS packet, it determines that another potential receiver j with a longer progress has accepted to forward the packet and node k switches to sleep for the duration of the communication.

The case for $N_p = 3$ priority regions is shown in Fig. 1. Based on their potential advancement, each feasible node corresponds to one of the three priority regions A_1, A_2, or A_3. The backoff scheme is also illustrated in Fig. 1, where the possible times when a CTS packet can be sent are shown. As an example, if a node in A_2 satisfies the initiative function, it first waits for CW_2 in addition to a random cw_2 value. Consequently, the node in A_2 can transmit a CTS packet only if no node in A_1 transmits a CTS packet.

When node i receives a CTS packet from a potential receiver, it determines that the receiver contention has ended and sends a DATA packet with the position of the winner node in the header. The CTS and DATA packets both inform the other contending nodes about the transmitter-receiver pair. Hence, other nodes stop contending and switch to sleep. In the case of two nodes sending CTS packets without hearing each other, the DATA packet sent by node i can resolve the contention. It may happen that multiple CTS packets from the same priority region can collide and a node from a lower priority region can be selected. XLP does not try to resolve this problem as this probability is very low since the contention region is already divided into multiple regions and the cost of trying to resolve this outweighs the gains.

Note that node i may not receive a CTS packet because of three reasons: 1) CTS packets collide, 2) there exist no potential neighbors with $\mathcal{I} = 1$, or 3) there exist no nodes in the feasible region. However, node i cannot differentiate these three cases by the lack of a CTS packet. Hence, the neighbors of node i send a keep alive packet after $\sum_{j=1}^{N_p} CW_j + cw$ if no communication is overheard. In this case, cw is a random number, where $cw \in [0, CW_{max}]$ and N_p is the number of priority regions as explained before. The existence of a keep alive packet notifies the sender that there exist nodes closer to the sink, but the initiative in (1) is not met for any of these nodes. With the reception of this packet, the node performs retransmission. However, if a keep alive packet is not received, the node continues retransmission in case there is a CTS packet collision. If no response is received after k retries, node i determines that a local minimum is reached and switches to an angle-based routing mode as explained next.

3.5 Angle-Based Routing

Since the routing decisions depend, in part, on the locations of the receivers, there may be cases where the packets reach a local minima. In other words, a node may not find any feasible nodes that are closer to the sink than itself. This problem is known as a communications void in geographical routing-based approaches and is generally resolved through face routing techniques [4], [10], [15], [16], [27]. Although localized, face routing necessitates a node to communicate with its neighbors to establish a planarized graph and construct routes to traverse around the void. This requires information exchange between the neighbors of a node. Since this communication increases the protocol overhead, we introduce a stateless solution to face routing, i.e., *angle-based routing* technique.

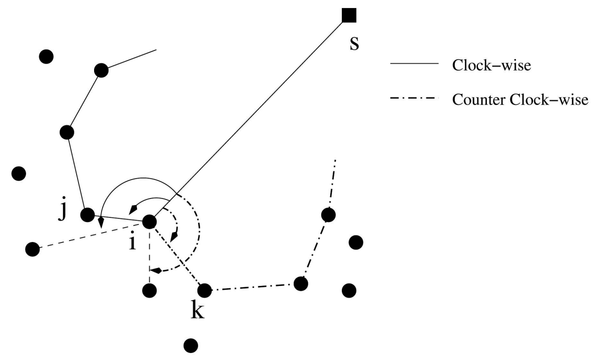

Fig. 2. Illustration of angle-based routing.

The main principle of angle-based routing can be seen in Fig. 2. When a packet reaches node i, which is a local minimum toward the sink, the packet has to be routed around the void either in clockwise direction (through node j) or in counterclockwise direction (through node k). Assume that lines are drawn between node i and sink s, as well as between node i and its neighbors. If we compare the angles between line i, s, and the other lines, angle $\angle sij$ (angle $\angle sik$) has the smallest angle in the counterclockwise (clockwise) routing direction. Using this geometric property, routes can be constructed around the void. Once a direction is set (clockwise or counterclockwise), the packet traverses around the void using the same direction. Hence, for angle-based routing, we introduce the term *traversal direction* to indicate this direction. Note that clockwise (counterclockwise) traversal direction refers to the traversal direction of the packets rather than the way the angles are measured.

When a node switches to angle-based routing mode, it also sets the traversal direction to clockwise and sends an RTS packet, which indicates both the routing mode and the traversal direction. The nodes that receive this packet calculate their angle relative to the source-sink direction. Denoting the angle by θ_{ij}, node j sets its contention window to $c\theta_{ij} + cw_i$, where cw_i is a random number and c is a constant.[3] The node with the smallest angle (hence, the smallest contention window) sends a CTS packet and the data communication takes place. This procedure is repeated until the packet reaches a local minimum. In this case, the traversal direction is set to counterclockwise and the procedure is repeated. Angle-based routing is terminated and the basic XLP is performed when the packet reaches a node that is closer to the sink than the node that initiated the angle-based routing. A sample route found by this algorithm is shown in Fig. 3, where the sink is denoted by s. Since node a is a local minimum, XLP switches to angle-based routing mode in clockwise direction. The packet is routed toward node c, where the traversal direction is changed and the packet reaches node d. Since node d is closer to the sink than node a, the angle-based routing mode is terminated and the packet is forwarded until node e using basic XLP. At node e, a local minimum is reached and the angle-based routing mode is used again. Finally, at node f, this mode is terminated since node f is closer to the sink than node e. The packet is routed from node f to sink s using basic XLP.

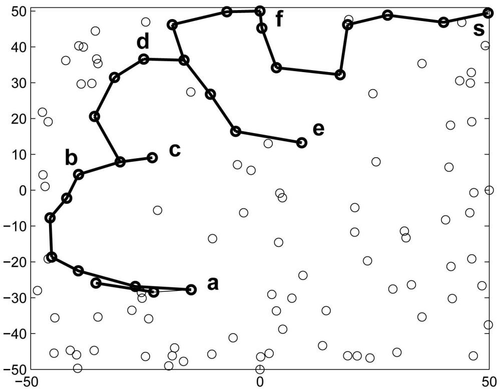

Fig. 3. Sample route created by angle-based routing.

The correctness of the angle-based routing protocol can be proved by proving that no loops are generated. It is well known that, according to the right-hand rule, traversing along a face prevents loops as long as the next face is correctly chosen [4]. In angle-based routing, nodes select their next hops according to the minimum angle between themselves and the previous nodes. This ensures that the packet always traverses on the edge of the face. Consequently, loops can only be created if the packet traverses through the initial face back to the initial sender. However, for this to occur, the packet should coincide with the direct line between the initial sender and the sink, which indicates that the packet reaches a node that is closer to the sink. This is a contradiction since, in this case, the protocol switches to geographical routing and the loops are prevented.

3.6 Local Cross-Layer Congestion Control

XLP incorporates a new hop-by-hop local cross-layer congestion control component, which is devised based on the buffer occupancy analysis presented here. The objective of this component is to perform hop-by-hop congestion control by exploiting the local information in the receiver contention and avoid the need for end-to-end congestion control. It also exploits the local reliability measures taken by the channel access functionality, and hence, does not necessitate traditional end-to-end reliability mechanisms.

A sensor node has two duties in WSNs, i.e., source duty and router duty. Accordingly, we consider two sources of traffic as an input to the buffer of each node: 1) *Generated packets:* The first source is the application layer, i.e., the sensing unit of a node, which senses the event and generates the data packets to be transmitted. The rate of the generated packets is denoted by λ_{ii}. 2) *Relay packets:* In addition to generated packets, as a part of its router duty, a node also receives packets from its neighbors to be forwarded to the sink due to multihop nature of sensor networks. The rate at which node i receives relay packets from node j is denoted by λ_{ji}.

The input rate to the buffer of node i is, hence, the combination of the input rates of these two types of packets. Since the sensor nodes utilize a duty cycle operation, the buffer occupancy of the nodes build up while they sleep because of the generated packets unless appropriate actions

[3] The constant can be selected according to the latency requirements and the density of the network.

are taken. The local cross-layer congestion control component of XLP has two main measures: 1) It regulates the congestion in router duty by letting sensor nodes participate in forwarding relay packets based on the current load of the node. 2) In source duty, it explicitly controls the rate of the generated packets.

We first analyze the upper bound for the total relay packet rate that will prevent congestion. Accordingly, a decision bound is derived for local congestion at each node. More specifically, this bound, denoted by λ_{relay}^{Th}, is used in the XLP initiative determination as presented in (1) in Section 3.

The overall input packet rate at node i, λ_i, can be represented as

$$\lambda_i = \lambda_{ii} + \lambda_{i,relay} = \lambda_{ii} + \sum_{j \in \mathcal{N}_i^{in}} \lambda_{ji}, \quad (2)$$

where λ_{ii} is the generated packet rate, λ_{ji} is the relay packet rate from node j to node i, $\mathcal{N}_i^{in}$ is the set of nodes from which node i receives relay packets, and $\lambda_{i,relay}$ is the overall relay packet rate of node i. Node i aims to transmit all the packets in its buffer, and hence, the overall output rate of node i is given by

$$\mu_i = (1 + e_i)(\lambda_{ii} + \lambda_{i,relay}), \quad (3)$$

where e_i is the packet error rate and $1 + e_i$ is used to approximate the retransmission rate since the routes are selected by considering a high SNR value through the initiative determination process. Note that, since the node retransmits the packets that are not successfully sent, the output rate is higher than the input rate.

According to (2) and (3), in a long enough interval, T_∞, the average time the node i spends in transmitting and receiving, is given by

$$\begin{aligned} T_{rx} &= \lambda_{i,relay} T_\infty T_{PKT}, \\ T_{tx} &= (1 + e_i)(\lambda_{ii} + \lambda_{i,relay}) T_\infty T_{PKT}, \end{aligned} \quad (4)$$

respectively, where T_{PKT} is the average duration to transmit a packet to another node including the medium access overhead.

To prevent congestion at a node, the generated and received packets should be transmitted during the time the node is active. Because of the duty cycle operation, on average, a node is active δT_∞ sec. Therefore,

$$\delta T_\infty \geq \big[(1 + e_i)\lambda_{ii} + (2 + e_i)\lambda_{i,relay}\big] T_\infty T_{PKT}. \quad (5)$$

Consequently, the input relay packet rate, $\lambda_{i,relay}$, is bounded by

$$\lambda_{i,relay} \leq \lambda_{i,relay}^{Th}, \quad (6)$$

where the relay rate threshold, $\lambda_{i,relay}^{Th}$, is given by

$$\lambda_{i,relay}^{Th} = \frac{\delta}{(2 + e_i) T_{PKT}} - \frac{1 + e_i}{2 + e_i} \lambda_{ii}. \quad (7)$$

The above analysis shows that, by throttling the input relay rate, congestion at a node can be prevented. This result is incorporated into XLP through a hop-by-hop congestion control mechanism, where nodes participate in routing packets as long as (6) is satisfied. The implementation of the inequality in (6) necessitates a node to calculate the parameters e_i, T_{PKT}, and λ_{ii}. To this end, the generated packet rate, λ_{ii}, is easily extracted from the rate of injected packets from the sensing boards to the communication module. The packet error rate, e_i, is stored as a moving average of the packet loss rate encountered by the node. Similarly, T_{PKT} is determined by using the delay encountered in sending the previous packet by the node. Consequently, each node updates these values after a successful or unsuccessful transmission of a packet.

According to (7), the relay rate threshold, $\lambda_{i,relay}^{Th}$, is directly proportional to the duty cycle parameter, δ. This suggests that the capacity of the network will decrease as δ is reduced. Moreover, the inequality in (6) ensures that the input relay rate of source nodes, i.e., nodes with $\lambda_{ii} > 0$, is lower than that of the nodes that are only relays, i.e., $\lambda_{ii} = 0$. This provides homogenous distribution of traffic load in the network, where source nodes relay less traffic.

The inequality given in (6) controls the congestion in the long term. However, in some cases, the buffer of a node can still be full due to short-term changes in the traffic. To prevent buffer overflow in these cases, the third inequality in (1) is used by the nodes to determine their initiative. More specifically, the inequality $\beta \leq \beta^{max}$ ensures that the buffer level, β, is lower than the threshold, β^{max}, which is the maximum buffer length of a node. Consequently, if a node's buffer is full, it does not participate in communication.

In addition to regulating the relay functionality as discussed above, the XLP local congestion control component also takes an active control measure by directly regulating the amount of traffic generated and injected into the network. During the receiver contention mechanism described in Section 3.4, node i may not receive any CTS packets but receive keep alive packets. In this case, node i decides that the network is congested. Accordingly, it reduces its transmission rate by decreasing the amount of traffic generated by itself. In other words, since the traffic injected by any node due to its router duty is controlled based on (6), the active congestion control is performed by controlling the rate of generated packets λ_{ii} at the node i.

In case of congestion, the XLP node reduces the rate of generated packets λ_{ii} multiplicatively, i.e., $\lambda_{ii} = \lambda_{ii} \cdot 1/\nu$, where ν is defined to be the transmission rate throttle factor. If there is no congestion detected, then the packet generation rate can be increased conservatively to prevent oscillation in the local traffic load. Therefore, the XLP node increases its generated packet rate linearly for each ACK packet received, i.e., $\lambda_{ii} = \lambda_{ii} + \alpha$. XLP adopts a rather conservative rate control approach mainly because it has two functionalities to control the congestion for both the source and the router duties of a sensor node. As the node decides to take part in the forwarding based on its buffer occupancy level and relay rate, it already performs congestion control as a part of the XLP's forwarding mechanism. Hence, the XLP node does not apply its active congestion control measures, i.e., linear increase and multiplicative decrease, to the *overall* transmission rate. Instead, only the generated packet rate, λ_{ii}, is updated.

Since the local congestion control is specific to certain regions and may not apply to the entire event area, nodes inside a congested region may reduce their transmission rates and the overall event reliability may still be met at the sink from the data from other nodes due to the sheer amount of correlated data flows as in [1]. Thus, instead of an inefficient end-to-end reliability mechanism, the local cross-layer congestion control exploits the local congestion control and reliability to maintain high network utilization and overall reliability in a distributed manner. In fact, this is also clearly observed in the performance evaluation results presented in Section 4.

3.7 XLP Duty Cycle Analysis

XLP employs a distributed duty cycle operation as described in Section 3.2. Hence, the choice of the duty cycle value, δ, is important for the performance of XLP. Accordingly, we investigate the effect of duty cycle on the network performance using an energy consumption analysis. In this respect, we investigate the energy consumed by the network for a packet sent to the sink as a function of the distance between the source and the sink.

The total energy consumed from a source node at distance D from the sink can be found as

$$E_{flow}(D) = E_{per\_hop}\ E[n_{hops}(D)], \tag{8}$$

where E_{per_hop} is the average energy consumed in one hop for transmitting a packet, and $E[n_{hops}(D)]$ is the expected hop count from a source at distance D to the sink given as [2]:

$$E[n_{hops}(D)] \simeq \frac{D - R_{inf}}{E[d_{next\_hop}]} + 1, \tag{9}$$

where $E[d_{next\_hop}]$ is the expected hop distance, which we have previously analyzed and derived in [30], [31] and R_{inf} is the approximated transmission range.

The energy consumed in one hop has three components as given by

$$E_{per\_hop} = E_{TX} + E_{RX} + E_{neigh}, \tag{10}$$

where E_{TX} is the energy consumed by the node transmitting the packet, E_{RX} is the energy consumed by the node receiving the packet, and E_{neigh} is the energy consumed by the neighbors of both the transmitter and receiver nodes. Similar energy consumption analysis has also been performed in the literature in a node-centric manner, which requires assumptions for the generated traffic, e.g., [25]. On the other hand, the effect of neighbor nodes has not been considered [12]. In our analysis, we investigate the energy consumption to transmit a single packet to the sink with the effect of neighbor nodes, which provides a clearer insight into the energy consumption.

To successfully transmit the packet, a pair of nodes need to complete the four-way handshaking. Assume that the distance between the pair of nodes is $d_h = E[d_{next\_hop}]$. Moreover, the probabilities to successfully receive a data packet and a control packet at this distance are $p_s^D(d_h)$ and $p_s^C(d_h)$, respectively.[4] When a transmitter node sends an RTS packet, it is received by the receiver node with probability $p_s^C(d_h)$ and the node replies with a CTS packet. If the CTS packet is received (also with probability $p_s^C(d_h)$), the transmitter node sends a DATA packet, and the communication is concluded with an ACK packet. In every failure event, the node begins retransmission. Therefore, the expected energy consumed by the transmitting node, E_{TX}, is

$$E_{TX} = \frac{K}{\left(p_s^C\right)^3 p_s^D}, \tag{11}$$

where

$$\begin{aligned} K = {} & E_{sense} + (p_s^C)^2\left[E_{tx}^R + E_{wait}^C + E_{rx}^C\right] \\ & + \left(1 - \left(p_s^C\right)^2\right)E_{t/o}^C + \left(p_s^C\right)^3 p_s^D\left[E_{tx}^D + E_{rx}^A\right] \\ & + \left(p_s^C\right)^2\left(1 - p_s^C p_s^D\right)E_{t/o}^A \end{aligned}$$

and E_{sense} is the energy consumption spent for sensing the region, E_{tx}^x and E_{rx}^x are the packet transmission and reception energies spent for packets, and the superscripts R, C, D, and A refer to RTS, CTS, DATA, and ACK packets, respectively. E_{wait}^{CTS} is the expected energy consumption for waiting for a receiver CTS, and $E_{t/o}$ is the energy consumed before the transmitter node times out, deciding that a suitable relay node does not exist. The two terms in (11), E_{wait}^C and $E_{t/o}^C$, are the only system-dependent terms. The expected waiting time for the next hop E_{wait}^C is calculated next.

According to the discussion in Section 3.4, on average, each node in priority region A_i waits in its priority slot for $CW_{max}/2$ on the average in addition to waiting for the previous priority slots. Denoting the probability that the next hop for node $i, \mathcal{N}_i$, exists in A_k by $P_i = P\{N_i = j,\ s.t.\ j \in A_k\}$, the average waiting time for the next hop is given by

$$E_{wait}^C = e_{rx}\left\{\sum_{i=1}^{N_P}\left[\left(\sum_{k=1}^{i-1} CW_k\right) + \frac{CW_{max}}{2}\right]P_i\right\}, \tag{12}$$

where

$$P_i = (1 - p_{[A(\gamma_{i-1}),\xi_{Th}]})p_{[A(\gamma_i),\xi_{Th}]}, \tag{13}$$

$p_{[A(\gamma_i),\xi_{Th}]} = 1 - p_i$, p_i is given in (11) in [31], e_{rx} is the energy consumption for receiving, and γ_k is the maximum distance from the sink for nodes in A_k. Using the same approach, the energy consumption of the receiver node can be found as shown in (14).

$$E_{RX} = \frac{1}{(p_s^C)^3 p_s^D}\left\{E_{rx}^R + E_{wait}^C + E_{tx}^C + E_{rx}^D + E_{rx}^A\right\}, \tag{14}$$

$$\begin{aligned} E_{Neigh} = {} & \frac{1}{(p_s^C)^2 p_s^D}\Bigg\{\rho\delta\left(\pi R_{inf}^2 - 2\right)p_s^C E_{rx}^R \\ & + (\rho\delta A(D, R_{inf}, D) - 2)\left(E_{wait}^C + E_{rx}^C + \frac{E_{rx}^D}{2}\right)\Bigg\}. \end{aligned} \tag{15}$$

The last term in (10), E_{neigh}, is the energy consumed by the neighbors of the transmitter and the receiver nodes, which is expressed in (15). The first term in the parenthesis in (15) is the energy consumption of the neighbors of the transmitter node, which consume energy for RTS packet reception. The second term models the remaining neighbors of the receiver nodes that listen only to the CTS message sent by the receiver node.

Finally, the probability that a packet is received is given by [33]

[4] We reasonably assume that the lengths of the RTS, CTS, and ACK packets are the same.

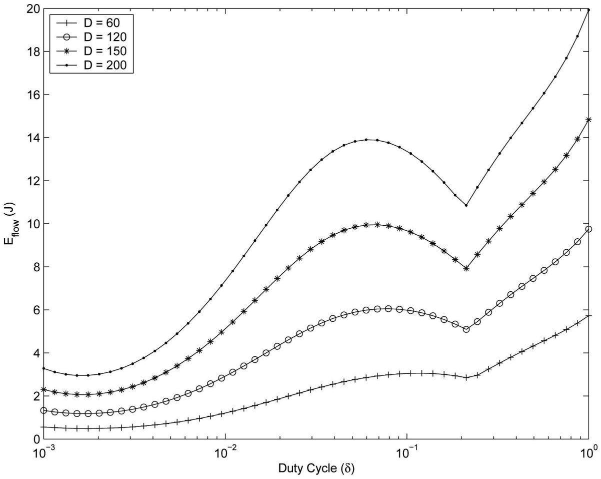

Fig. 4. Average energy consumption versus duty cycle for different values of D.

$$p_s = \left(1 - \frac{1}{2} e^{-\frac{\xi}{1.28}}\right)^{16l}, \tag{16}$$

where Mica2 architecture is assumed with Manchester encoding, ξ is the received signal to noise ratio (SNR), and l is the packet length in bits, which is l_C and l_D for p_s^C and p_s^D, respectively.

Using (11), (14), (15), and (16) in (10), the overall energy consumption of a flow can be found. Using numerical integration methods, the effect of distance, D, on the energy consumption of a flow is found and shown in Fig. 4. Considering Fig. 4, the energy consumption of a flow is minimal for $\delta \sim 0.002$. However, in relatively small-sized networks of <1,000 nodes, this operating point may not provide connectivity in the network. On the other hand, note also that the energy consumption has a local minima around $\delta = 0.2$. We will also show by comprehensive performance evaluations in Section 4 that this value is a suitable operating point for XLP in terms of energy efficiency.

4 Performance Evaluation

To gain more insight into the protocol operation, we first investigate the effects of XLP parameters on the overall network performance. Then, we present a comparative study between XLP and five different layered protocol suites consisting of the state-of-the-art protocols and a cross-layer protocol. Finally, we discuss the overall communication complexity of these solutions. We evaluate XLP and various protocol suites in a cross-layer simulator (XLS) developed at our laboratory in C++. XLS consists of a realistic channel model based on [33] and ns-2 and an event-driven simulation engine. The channel errors, packet collisions, and energy consumption for communication are accurately modeled based on ns-2. We present simulation results for a sensor topology of 300 nodes randomly deployed in a $100 \times 100\ \mathrm{m}^2$ sensor field. The sink is located at the coordinates (80,80). The simulation parameters for both sensor nodes and the communication suites are given in Table 1. In each simulation, an event occurs in an *event area* located at coordinates (20,20) with an event radius of 20 m. Each source node reports its event information to the sink. To investigate the effect of duty cycle, each simulation is performed for duty cycle values of $\delta \in [0.1, 1]$. Each simulation lasts for 300 s and the average of 10 trials for each of 10 different random topologies are shown along with their 95 percent confidence intervals.

TABLE 1
Simulation Parameters

Parameter	Value	Parameter	Value
Re-tx. Limit	7	P_t	5 dBm
ν	2	PL(d_0)	55 dB
α	0.125	P_n	-105 dBm
Buffer Length	30	d_0	1m
$l_{control}$	20 bytes	n	3
l_{data}	100 bytes	σ	3.8
Frame Length	5s	$T_{coherence}$	16 ms
Energy Threshold	100 μJ	E_{rx}	13.5 mW
ξ_{Th}	10 dB	E_{tx}	24.75 mW
T_{sss}	5s	E_{sleep}	15 μW

In the evaluations, we investigate the following performance metrics:

- *Throughput* is the number of bits per second received at the sink. In calculating this metric, only unique packets are considered since multiple copies of a packet can be received at the sink for certain protocols.
- *Goodput* is the ratio between the total number of unique packets received at the sink and the total number of packets sent by all the source nodes. As a result, the overall communication reliability of the suites is investigated.
- *Energy Efficiency* is the most important metric in WSNs. We consider the average energy consumption per unique packet that is received at the sink, which can be considered the inverse of energy efficiency. Hence, a lower value refers to a more energy-efficient communication.
- *Number of Hops* is the number of hops each received packet traverses to reach the sink. This metric is used to evaluate the routing performance of each suite.
- *Latency* is the time it passes between the time a packet is generated at a source node and the time it is received at the sink. This delay accounts for the queuing delay and the contention delay at the nodes as well as specific protocol operation overhead.

4.1 XLP Parameters

The parameters that affect the XLP operation are angle-based routing, SNR threshold, ξ_{Th}, and duty cycle, δ. We present the effects of these parameters on the XLP performance in this section.

The effect of angle-based routing is shown in Fig. 5, where the route failure rate versus duty cycle parameter δ is shown for XLP with and without angle-based routing. In these experiments, a snapshot of the network is considered and the routes are found considering this topology. The route failure is the ratio of the number of unsuccessful routes between each node in the network and the number of all possible routes. The results show that route failure rate increases as the duty cycle parameter δ is decreased. On the

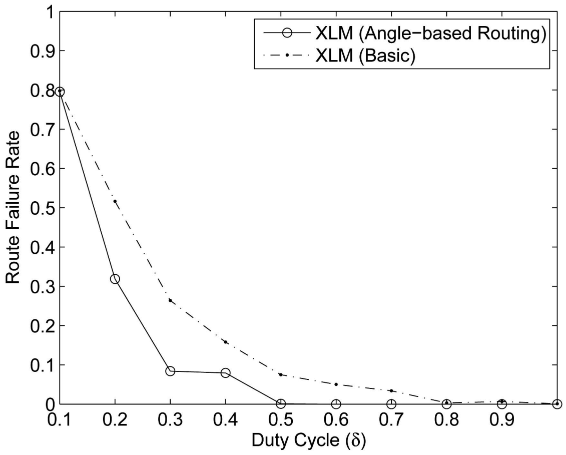

Fig. 5. Route failure rate for XLP with and without angle-based routing.

other hand, angle-based routing limits the route failure rate to less than 10 percent for $\delta \geq 0.3$. This leads to up to a 70 percent decrease in the failure rate. Note that the failure rate of XLP with angle-based routing also increases as δ is further decreased since the probability that at any given time the network is partitioned increases.

In Fig. 6a, the total throughput received at the sink is shown. The x-axis shows the duty cycle δ and the throughput is shown for different SNR threshold, ξ_{Th}, values. The network throughput increases as the duty cycle δ is increased. An increase in the duty cycle results in an increase in the number of nodes that are active at a given time. Consequently, the capacity of the network increases. This fact is also evident from our buffer occupancy analysis in Section 3.6. The effect of the SNR threshold, ξ_{th}, is also shown in Fig. 6a. The first curve in the figure, i.e., No ξ_{Th}, is the case where the first condition in (1) is not implemented. In other words, nodes contend for participating in routing irrespective of the received SNR value. It can be observed that increasing the SNR threshold, ξ_{Th}, improves the network throughput up to a certain ξ_{Th}. Above this value, the network throughput degrades. This shows that a very conservative operation of XLP leads to performance degradation.

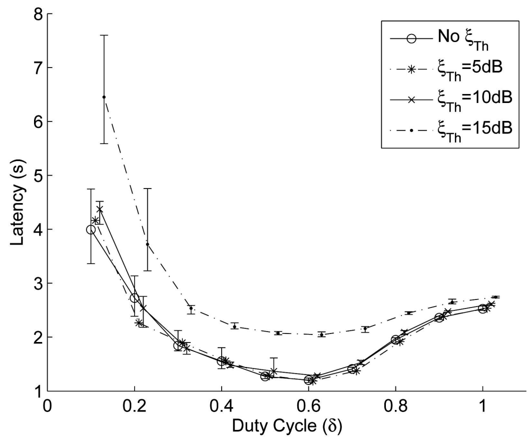

Fig. 7. Average latency versus duty cycle for different values of ξ_{Th}.

In Fig. 6b, the goodput performance is shown. Accordingly, XLP provides reliability above 90 percent for $\xi_{Th} \leq 10dB$. The decrease in goodput at $\delta = 0.1$ is due to the fact that the connectivity of the network cannot be maintained at all times. Moreover, for $\xi_{Th} = 15dB$, the goodput decreases to 0.7 as the duty cycle is decreased. This is due to the fact that potential receivers with the desired channel quality cannot be found and the reliability of the XLP degrades. For high duty cycle ($\delta > 0.7$), a slight decrease in goodput is observed for $\xi_{Th} < 15dB$. This accounts for the increased contention in the network since a higher number of nodes are active for participation in routing at a given time. In the case for $\xi_{Th} = 15dB$, since a fewer number of nodes are selected for contention in participation, collisions are limited and the goodput is not affected.

In Fig. 7, the end-to-end latency is shown, which reveals that increasing SNR threshold, ξ_{Th}, improves the end-to-end latency performance up to a certain ξ_{Th} value. $\xi_{Th} = 10dB$ results in the lowest latency. It is also interesting to note that there is a suitable operating point for duty cycle δ considering end-to-end latency ($\delta \sim 0.6$). Above this value, end-to-end

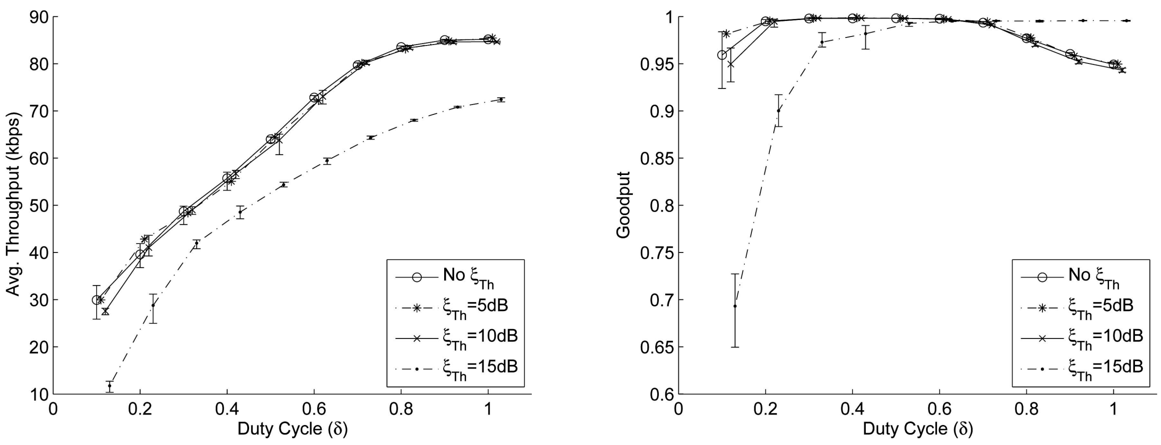

(a) (b)

Fig. 6. (a) Average throughput and (b) average goodput versus duty cycle for different values of ξ_{Th}.

delay starts to increase because of the increase in receiver-based contention. Since, for all above performance metrics, $\xi_{Th} = 10dB$ results in the most efficient performance, we use this value in the following comparative evaluations.

4.2 Comparative Evaluation

In this section, we compare the performance of the XLP with five different layered protocol architectures and a cross-layer protocol. We first identify the protocol configurations implemented in our study along with the implementation issues. Then, we present the results of our comparative evaluation for networks with and without duty cycle operation. The complexity issues are also discussed.

4.2.1 Protocol Configurations

The protocol configurations implemented for the comparative evaluation are as follows:

Flooding. This configuration serves as the baseline for the other configurations. Each node broadcasts its packet and the nodes that are closer to the sink rebroadcast this packet until it reaches the sink. At the MAC layer, a CSMA-type broadcast mechanism is used. No retransmission mechanism is used. At the transport layer, packets are injected at a constant rate and no rate control is used. The results shown include the unique packets received at the sink.

[GEO]: Geographical Routing + CC-MAC + ESRT. This protocol configuration is composed of ESRT [1], geographical routing [24], and CC-MAC [29] at transport, routing, and MAC layers, respectively. The CC-MAC protocol is implemented using $r_{corr} = 7m$, and $T_{SSS} = 5s$. For routing, *distance-based blacklisting* [24] is used such that the nodes in the farthest 20 percent of the radio range are blacklisted and the next closest node to the sink is selected as the next hop.

[PRR]: PRR-based Geographical Routing + CC-MAC + ESRT. This protocol configuration is similar to *GEO* with the exception that the routing decisions are based on the channel quality of each node with its neighbors. The channel quality is measured in terms of the packet reception rate (PRR) as discussed in [24]. The node that maximizes the *PRR* × *geographical advancement* product is selected as the next hop.

[PRR-SMAC]: PRR-based Geographical Routing + SMAC + ESRT. This protocol configuration is similar to *PRR* with the MAC layer replaced by the SMAC protocol [32]. In this configuration, the duty cycle operation proposed in [32] is implemented instead of the distributed duty cycle operation.

[DD-RMST]: Directed Diffusion + RMST. This case consists of RMST [26], directed diffusion [14], and the CSMA scheme. The RMST protocol is implemented with hop-by-hop recovery and caching, and no link-layer ARQ is used at the link layer as presented in [26]. *DD-RMST* is used in the comparative evaluations for operation without duty cycle, i.e., $\delta = 1$.

[ALBA-R]. The cross-layer ALBA-R protocol [3] is also included in the analysis since it represents many of the state-of-the-art concepts in cross-layer communication in WSNs and has been shown to outperform the MACRO protocol [9]. Since ALBA-R does not consider rate control, three different traffic rates are investigated: $\lambda = \{3, 4, 6.25\}$ pkts/s with a Poisson traffic according to [3]. Maximum values for QPI and GPI are selected as 20 and 3, respectively, since 20 is the buffer length and 3 is also employed in [3]. The rainbow mechanism uses four colors and the results after this mechanism converges are shown.

XLP. Our proposed cross-layer protocol (XLP) is implemented according to the protocol description in Section 3 with SNR threshold $\xi_{Th} = 10dB$.

It is important to note that the existing protocols that we have implemented in the layered suites are usually proposed considering only their related layers with reasonable assumptions about the other layers. As an example, in the geographical routing protocol [24], each node is assumed to know the locations of its neighbors. However, the actual implementation and operation of such an information exchange procedure is important especially when comparing these solutions to the proposed XLP solution. In that sense, XLP does not require that a node has location knowledge about each of its neighbors. Instead, each node participates in communication according to *its* own location. Consequently, an explicit information exchange between each neighbor is not required for XLP. In conventional geographical routing protocols, however, this constitutes a major overhead in terms of both communication and storage. Moreover, since duty cycle is deployed in our solution, each neighbor of a node may not always be active. Hence, in order for each protocol to work together in the protocol suites, we have made the following implementation modifications.

Accordingly, in *GEO, PRR*, and *PRR-SMAC*, each node broadcasts a beacon to inform its position and the remaining time to sleep. This beacon is sent at the beginning of each sleep frame when a node wakes up. Each neighbor that receives this beacon determines that the specific node will be active for the duration specified in the beacon. In the case of *PRR* and *PRR-SMAC*, this beacon also serves as a channel quality indicator. To optimize the network performance, in *GEO* and *PRR*, the beacons are piggybacked if there is a packet in the queue. In *PRR-SMAC*, a pairwise cross layering is used and the routing beacons are sent with the SYNC packets. Similarly, SYNC packets are piggybacked if there is a packet in the queue.

We have indicated that *DD-RMST* is used only for operation without duty cycle, i.e., $\delta = 1$, since neither directed diffusion nor RMST considers duty cycle operation [14], [26]. Therefore, the *DD-RMST* protocol configuration is evaluated only for $\delta = 1$ and shown as a single point in the figures for fairness and completeness of the evaluations.

We next present the results for operation with duty cycle, by changing the duty cycle δ from 0.1 to 1 in Section 4.2.2. The lines for each protocol are shifted slightly from each other with respect to the original duty cycle values (x-axis) to clearly show the confidence intervals. We represent the results for the evaluated protocols selectively to improve clarity in the figures.

4.2.2 Results

In Fig. 8a, the throughput comparison is presented. The throughput achieved by XLP is up to 55 percent higher than that of the layered protocol suites. This shows the clear advantage of using a cross-layer approach that governs the functionalities of three traditional layers. In the layered protocol suites, the cross-layer information is not efficiently

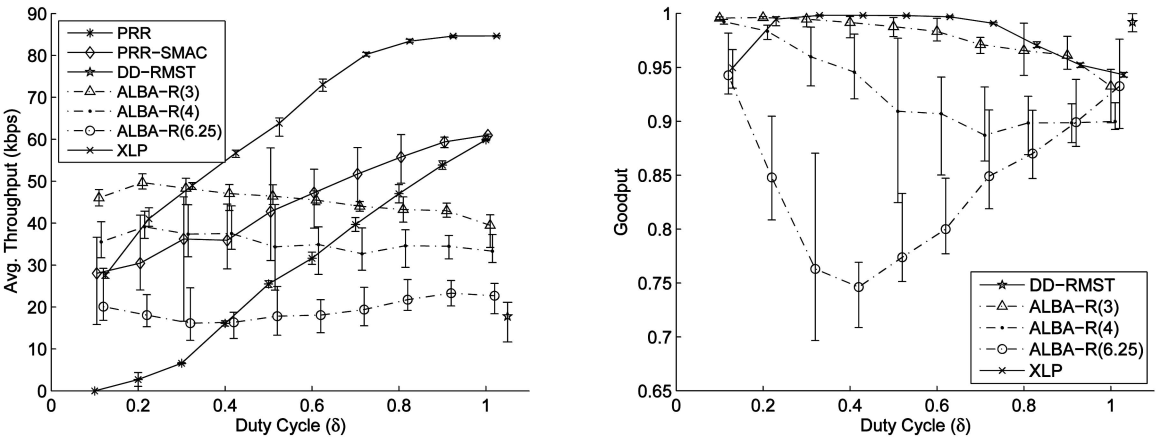

(a)

(b)

Fig. 8. (a) Average throughput and (b) average goodput versus duty cycle for different values of ξ_{Th}.

exploited for each functionality. For example, in *PRR* and *PRR-SMAC*, route selection is only performed based on location information and link quality, whereas the congestion level at a specific node is not considered. Another important result emerges in the comparison among XLP, *PRR*, and *PRR-SMAC*. *PRR* uses CC-MAC at the MAC layer. CC-MAC results in smaller number of nodes to send information as a representative of all the nodes in that area [29]. However, SMAC [32] does not exploit this property and all the nodes inside an event area send information to the sink. This results in an increase of almost three times in the number of source nodes. The higher throughput value of *PRR-SMAC* compared to *PRR* can be explained with this fact. However, XLP still outperforms *PRR-SMAC* in terms of total throughput, although a fewer number of nodes send information, which shows that the network capacity is exploited in a more efficient manner.

XLP more than doubles the throughput achieved by ALBA-R for duty cycle values $\delta \leq 0.3$. This is mainly because of the significant delay incurred at heach hop because of the scanning mechanism of ALBA-R. XLP, on the other hand, has a fixed delay for relay contention. Moreover, as the traffic rate increases from 3 to 6.25 pkts/s, the throughput of ALBA-R is halved. As the traffic load increases, the average QPI values of the nodes in the network increases. Consequently, a node spends a larger amount of time scanning the QPI values until a suitable neighbor is found. On the other hand, XLP employs a hop-by-hop congestion control mechanism to select nodes with lower queue occupancy in a shorter time. If the network becomes congested, traffic load is relieved through the source rate control mechanism. When the duty cycle value and the date rate are low ($\delta \leq 0.2$ and $\lambda = 3$ pkt/s), ALBA-R provides higher throughput compared to XLP. When the duty cycle is low, the possibility of finding an active next hop at a given time interval decreases. Since ALBA-R is a more persistent protocol beacuse of the longer QPI and GPI scanning mechanism, this protocol can establish routes when the traffic rate is low. However, since the networks cannot accomodate higher rates at low duty cycle values and ALBA-R does not probide a rate control mechanism, its throughput is lower than that of XLP for higher traffic rates.

Note that the total throughput achieved by *DD-RMST* is significantly lower than XLP ($\sim$3.7 times), *PRR-SMAC* ($\sim$2.4 times), and *PRR* ($\sim$2.3 times), and comparable to *Flooding* (not shown here, see [2]). This is due to two main reasons. First, the additional traffic created for recovering the lost packets increases the contention and decreases the capacity of the network. Second, the control packets of directed diffusion, i.e., the interest and exploratory packets, constitute a significant amount of traffic due to their broadcast nature.

The goodput is shown in Fig. 8b, where *DD-RMST*, *ALBA-R*, and XLP are shown since they consistently provide higher goodput than other protocols. Irrespective of the duty cycle value, δ, both cross-layer protocols XLP and ALBA-R ($\lambda = 3$), provide goodput higher than 90 percent. The cross-layer communication paradigm of the XLP that is adaptive to the network topology enables such high performance even when the network operates at low duty cycle. Coupled with the high throughput of XLP as shown in Fig. 8a, our cross-layer approach enables highly efficient communication. Moreover, *DD-RMST* provides 100 percent reliability while XLP and ALBA-R result in a reliability of 94 and 93 percent, respectively, for operation without duty cycle, i.e., $\delta = 1$. Note that the RMST protocol uses hop-by-hop recovery with negative acknowledgments to request missing packets. On the other hand, XLP aims to first prevent link losses by constructing noncongested, high-quality paths and then ensures high reliability by hop-by-hop ARQ technique. ALBA-R also employs a similar approach by selecting nodes with lower traffic load as the next hop. This approach results in reliability comparable to RMST at a significantly lower cost, as we will discuss next. ALBA-R results in 5 percent higher goodput for $\delta = 0.1$ and $\lambda \leq 4$ pkts/s. This is related to the higher persistency of the protocol than XLP. However, as the traffic load increases, goodput of ALBA-R decreases by 5-25 percent because of the lack of congestion control and the corresponding buffer overflows. Since source nodes do not throttle the injected traffic, intermediate nodes start to drop these packets if they cannot find the next hop with $QPI < QPI_{max}$. Since it results in the best performance, we show the results for $\lambda =$ 3 pkts/s for ALBA-R in the following figures. It is important

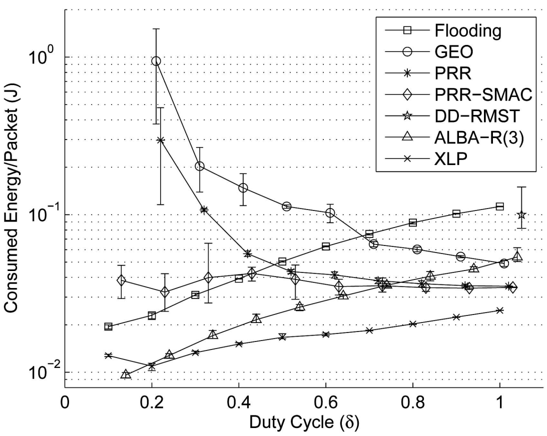

Fig. 9. Average energy consumption per packet versus duty cycle for different values of ξ_{Th}.

to note that it is an important challenge for the ALBA-R protocol to find the suitable traffic rate.

The decrease in reliability for the other layered protocol suites is mainly because of the significant number of packet drops due to retransmission time-outs [2].[5] This suggests that nodes cannot find their intended next hops due to either low channel quality or because the intended nodes switch to sleep state before receiving any packets. This is exacerbated especially in the case of low duty cycle. As a result, the reliability of the network is significantly hampered.

In Fig. 9, the energy consumption per packet is shown, where the values for *GEO* and *PRR* at $\delta = 0.1$ are not shown since no packets are received at the sink. XLP consumes 28-66 percent less energy per packet compared to the most energy-efficient layered protocol suite, *PRR-SMAC*. Similarly, XLP is 14-54 percent more energy: efficient compared to ALBA-R for duty cycle values ($\delta \geq 0.2$). This difference is mainly because of the periodic broadcast of beacon packets in *GEO* and *PRR*, and SYNC packets in *PRR-SMAC*. Furthermore, the significant percentage of retransmission timeouts indicates significant energy wastage due to packets that cannot be transmitted to the sink. Since the network and MAC layers operate independently, a node chosen by the routing layer cannot be reached by the MAC protocol immediately due to the duty cycle operation. This delay leads to increased energy consumption.

An interesting result is the threefold higher energy consumption of *DD-RMST* compared to XLP. Although this configuration provides 100 percent reliability as shown in Fig. 8b, the layered structure of the routing, transport, and MAC functionalities results in a high penalty. The routing layer, i.e., directed diffusion, incurs significant amount of overhead in order to maintain end-to-end paths between sources and the destination. On the contrary, XLP employs an adaptive routing technique that provides an energy-efficient path in terms of both link quality and energy consumption distribution.

The energy consumption of ALBA-R is up to 54 percent higher than that of XLP for $\delta > 0.1$. ALBA-R results in 32 percent lower energy consumption for $\delta = 0.1$ compared to XLP. As the duty cycle increases, the number of active nodes increases. As a result, due to continuous polling of QPI values in ALBA-R, the neighbors of a node consume higher amount of energy. Furthermore, since the probability of finding nodes with the same QPI increases, these nodes also go through GPI scanning. Although ALBA-R aims to transmit multiple packets after a next hop is found, the cost of finding the next hop is higher. Instead, XLP resolves contention by the integration of a next hop determination mechanism to the backoff mechanism of the contending nodes, which results in higher energy efficiency. Another important observation in Fig. 9 is that the energy consumption per packet for XLP has a minimum at $\delta = 0.2$. This is consistent with the mathematical analysis provided in Section 3.7.

The advantages of using a separate routing layer in the layered protocol suites can be seen in Fig. 10a, where the average hop count is shown. *GEO, PRR, PRR-SMAC*, and *DD-RMST* result in a fewer number of hops than XLP (for *GEO* and *PRR* performance, see [2]). This is due to the fact that the routing algorithms in these layered protocol suites aim to find the smallest number of hops. This result may be incorporated as a disadvantage of XLP when only the routing layer is taken into account. However, the overall performance of XLP reveals that maximizing the routing layer performance alone does not provide efficient communication in WSNs. In other words, while a smaller number of hops might be optimal in terms of *routing* efficiency, other effects such as link quality, contention level, congestion level, and overall energy consumption necessitate a cross-layer approach in route selection for *overall* efficiency.

Furthermore, as shown in Fig. 10b, XLP provides end-to-end latency comparable to *Flooding* and *GEO*. Furthermore, ALBA-R results in up to $\sim$2.8 times higher latency, which is also reported in [3]. In Fig. 10b, the cost of the high reliability of *DD-RMST* results in significantly high latency due to the end-to-end reliability mechanism. Note that the end-to-end latency of XLP more than doubles for low δ. This is due to the fact that sender nodes cannot find any neighbors that satisfy the constraints in (1) discussed in Section 3.

4.2.3 Implementation Complexity

In addition to the performance of our XLP module in terms of network metrics, the complexity and implementation issues of cross-layer design are also important. In this section, we provide a qualitative comparison of cross-layer design and layered protocol architectures implemented in our simulation environment.

One of the major advantages of cross-layer design for communication protocols is the implementation efficiency. In a traditional layered protocol architecture, each layer has clear boundaries. This layered structure leads to computation delays due to the sequential handling of a packet. For example, in TinyOS [34], each layer has to wait for the lower layers to process the packet since a single buffer is used for a packet for all layers. XLP, however, blends the functionalities of traditional medium access, routing, and congestion control into a unified cross-layer communication module by considering physical layer and channel effects. Hence, these functionalities are performed as a whole and the overall protocol efficiency can be improved using XLP.

[5] Not shown here for space considerations.

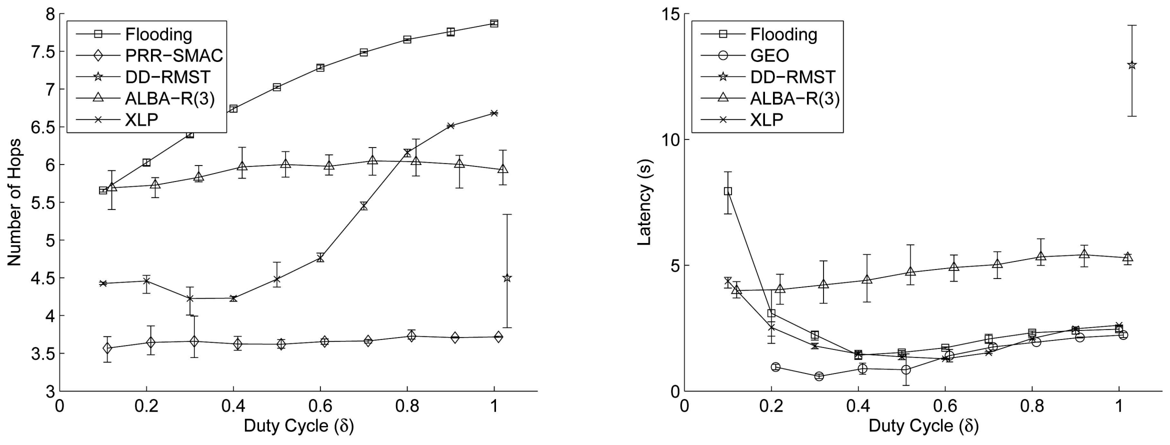

(a) (b)

Fig. 10. (a) Average hop count and (b) average latency versus duty cycle for layered protocol suites and XLP.

In addition to the simulation performance, the implementation issues are also important for a complete comparison. As explained in Section 3, XLP does not require any tables or extra buffer space for routing and congestion control functionalities. The routing is performed based on receiver initiatives, which eliminates the need for a routing table at each node. The implementation of XLP is both simple and compact. On the other hand, in *PRR-SMAC*, the *SMAC* protocol maintains a schedule table for each of the one-hop neighbors to provide synchronized sleeping cycles. Similarly, in *DD-RMST*, at the routing layer, each node has to implement a reinforcement table for each source indicating the next hop in the reinforced path. In case a node is a source node, it also has to keep track of multiple neighbors which have a path to the sink for exploratory messages. At the transport layer, RMST [26] requires a separate queue to cache data locally to support loss recovery at all hops. These requirements, due to either layered operation of the protocol stack or the internal protocol structure at each layer, place a burden on memory space for communication in sensor nodes. Compared to the layered protocol stacks, ALBA-R requires smaller code space because of the cross-layer MAC/routing operation. However, compared to XLP, ALBA-R necessitates large state information to be stored in each node because of the QPI and GPI scanning process.

The extra space required by the communication stacks limits the available space to develop new applications for sensor networks. On the other hand, the careful use of code space and cross-layer implementation of communication functionalities in XLP provides a more efficient operation in WSNs. When coupled with the noticeably better communication performance as discussed in Section 4.2.2, XLP becomes a successful candidate for communication protocols in WSNs.

5 Conclusion

Recently, cross layering in designing a communication stack such that state information flows throughout the stack has been investigated. Recent work on WSNs [11], [13] also reveals that cross-layer integration techniques result in significant energy gains. In this paper, we propose a novel *initiative determination* concept that allows many communication and networking functionalities be implemented in a single protocol. Accordingly, the cross-layer procotcol (XLP) is proposed to provide the functionalities of medium access, routing, and congestion control. Based on the initiative determination concept, XLP serves as a proof of concept and performs receiver-based contention, initiative-based forwarding, local congestion control, and distributed duty cycle operation to realize efficient and reliable communication in WSNs. Analytical performance evaluation and simulation experiment results show that XLP significantly improves the communication performance and outperforms the traditional layered protocol architectures in terms of both network performance and implementation complexity.

The ultimate goal in the cross-layer design technique is to develop a single communication module that is responsible for the functionalities of each networking layer. The initiative determination concept developed in this work is the first step in this approach to replace the entire traditional layered protocol architecture that has been used so far in WSNs so that both the information and the functionalities of traditional communication layers are blended in a single module. Consequently, the future work for our research includes the investigation of various networking functionalities such as adaptive modulation, error control, and topology control in a cross-layer fashion to develop a unified cross-layer communication module.

Acknowledgments

This work is supported by the US National Science Foundation under contract CNS-0519841.

References

[1] Ö.B. Akan and I.F. Akyildiz, "Event-to-Sink Reliable Transport in Wireless Sensor Networks," *IEEE/ACM Trans. Networking*, vol. 13, no. 5, pp. 1003-1016, Oct. 2005.

[2] I.F. Akyildiz, M.C. Vuran, and O.B. Akan, "A Cross-Layer Protocol for Wireless Sensor Networks," *Proc. Conf. Information Sciences and Systems (CISS '06)*, Mar. 2006.

[3] P. Casari, M. Nati, C. Petrioli, and M. Zorzi, "Efficient Non Planar Routing around Dead Ends in Sparse Topologies Using Random Forwarding," *Proc. IEEE Int'l Conf. Comm. (ICC '07)*, June 2007.

[4] D. Chen and P.K. Varshney, "A Survey of Void Handling Techniques for Geographic Routing in Wireless Networks," *IEEE Comm. Surveys and Tutorials,* vol. 9, no. 1, pp. 50-67, 2007.

[5] M. Chiang, "To Layer or Not to Layer: Balancing Transport and Physical Layers in Wireless Multihop Networks," *Proc. IEEE INFOCOM,* vol. 4, pp. 2525-2536, Mar. 2004.

[6] M. Chiang, "Balancing Transport and Physical Layers in Wireless Multihop Networks: Jointly Optimal Congestion Control and Power Control," *IEEE J. Selected Areas Comm.,* vol. 23, no. 1, pp. 104-116, Jan. 2005.

[7] S. Cui, R. Madan, A. Goldsmith, and S. Lall, "Joint Routing, MAC, and Link Layer Optimization in Sensor Networks with Energy Constraints," *Proc. IEEE Int'l Conf. Comm. (ICC '05),* vol. 2, pp. 725-729, May 2005.

[8] S. De et al., "An Integrated Cross-Layer Study of Wireless CDMA Sensor Networks," *IEEE J. Selected Areas Comm.,* vol. 22, no. 7, pp. 1271-1285, Sept. 2004.

[9] D. Ferrara, L. Galluccio, A. Laonardi, G. Morabito, and S. Palazzo, "MACRO: An Integrated MAC/Routing Protocol for Geographical Forwarding in Wireless Sensor Networks," *Proc. IEEE INFOCOM,* Mar. 2005.

[10] M. Fraser, E. Kranakis, and J. Urrutia, "Memory Requirements for Local Geometric Routing and Traversal in Digraphs," *Proc. Canadian Conf. Computational Geometry (CCCG '08),* Aug. 2008.

[11] V.C. Gungor, M.C. Vuran, and O.B. Akan, "On the Cross-Layer Interactions between Congestion and Contention in Wireless Sensor and Actor Networks," *Ad Hoc Networks J.,* vol. 5, no. 6, pp. 897-909, Aug. 2007.

[12] J. Haapola, Z. Shelby, C.A. Pomalaza-Ráez, and P. Mähönen, "Cross-Layer Energy Analysis of Multi-Hop Wireless Sensor Networks," *Proc. European Workshop Wireless Sensor Networks,* Feb. 2005.

[13] L. van Hoesel, T. Nieberg, J. Wu, and P.J.M. Havinga, "Prolonging the Lifetime of Wireless Sensor Networks by Cross-Layer Interaction," *IEEE Wireless Comm.,* vol. 11, no. 6, pp. 78-86, Dec. 2004.

[14] C. Intanagonwiwat, R. Govindan, D. Estrin, J. Heidemann, and F. Silva, "Directed Diffusion for Wireless Sensor Networking," *IEEE/ACM Trans. Networking,* vol. 11, no. 1, pp. 2-16, Feb. 2003.

[15] B. Karp and H.T. Kung, "GPSR: Greedy Perimeter Stateless Routing for Wireless Networks," *Proc. ACM MobiCom,* pp. 243-254, Aug. 2000.

[16] B. Leong, S. Mitra, and B. Liskov, "Path Vector Face Routing: Geographic Routing with Local Face Information," *Proc. IEEE Int'l Conf. Network Protocols (ICNP '05),* Nov. 2005.

[17] X. Lin and N.B. Shroff, and R. Srikant, "A Tutorial on Cross-Layer Optimization in Wireless Networks," *IEEE J. Selected Areas Comm.,* vol. 24, no. 8, pp. 1452-1463, June 2006.

[18] X. Lin and N.B. Shroff, "The Impact of Imperfect Scheduling on Cross-Layer Congestion Control in Wireless Networks," *IEEE/ACM Trans. Networking,* vol. 14, no. 2, pp. 302-315, Apr. 2006.

[19] S. Liu, K.-W. Fan, and P. Sinha, "CMAC: An Energy Efficient MAC Layer Protocol Using Convergent Packet Forwarding for Wireless Sensor Networks," *Proc. Int'l Conf. Sensor and Ad Hoc Comm. and Networks (SECON '07),* June 2007.

[20] D. Moore, J. Leonard, D. Rus, and S. Teller, "Robust Distributed Network Localization with Noisy Range Measurements," *Proc. ACM Int'l Conf. Embedded Networked Sensor Systems (Sensys '04),* Nov. 2004.

[21] P.R. Morin, "Online Routing in Geometric Paths," PhD thesis, School of Computer Science, Carleton Univ., 2001.

[22] D. Pompili, M.C. Vuran, and T. Melodia, "Cross-Layer Design in Wireless Sensor Networks," *Sensor Network and Configuration: Fundamentals, Techniques, Platforms, and Experiments,* M.P. Mahalik, ed., Springer-Verlag, Aug. 2006.

[23] L. Savidge, H. Lee, H. Aghajan, and A. Goldsmith, "Event-Driven Geographic Routing for Wireless Image Sensor Networks," *Proc. Conf. COGnitive Systems with Interactive Sensors (COGIS '06),* Mar. 2006.

[24] K. Seada, M. Zuniga, A. Helmy, and B. Krishnamachari, "Energy-Efficient Forwarding Strategies for Geographic Routing in Lossy Wireless Sensor Networks," *Proc. ACM Int'l Conf. Embedded Networked Sensor Systems (Sensys '04),* Nov. 2004.

[25] P. Skraba, H. Aghajan, and A. Bahai, "Cross-Layer Optimization for High Density Sensor Networks: Distributed Passive Routing Decisions," *Proc. Int'l Conf. Ad-Hoc Networks and Wireless (Ad-Hoc Now '04),* July 2004.

[26] F. Stann and J. Heidemann, "RMST: Reliable Data Transport in Sensor Networks," *Proc. IEEE Workshop Sensor Networks Protocols and Applications (SNPA '03),* pp. 102-112, Apr. 2003.

[27] J. Urrutia, "Local Solutions for Global Problems in Wireless Networks," *J. Discrete Algorithms,* no. 5, vol. 3, pp. 395-407, Sept. 2007.

[28] M.C. Vuran, Ö.B. Akan, and I.F. Akyildiz, "Spatio-Temporal Correlation: Theory and Applications for Wireless Sensor Networks," *Computer Networks J.,* vol. 45, no. 3, pp. 245-261, June 2004.

[29] M.C. Vuran and I.F. Akyildiz, "Spatial Correlation-Based Collaborative Medium Access Control in Wireless Sensor Networks," *IEEE/ACM Trans. Networking,* vol. 14, no. 2, pp. 316-329, Apr. 2006.

[30] M.C. Vuran and I.F. Akyildiz, "Cross-Layer Analysis of Error Control in Wireless Sensor Networks," *Proc. IEEE Int'l Conf. Sensor and Ad Hoc Comm. and Networks (SECON '06),* Sept. 2006.

[31] M.C. Vuran and I.F. Akyildiz, "Error Control in Wireless Sensor Networks: A Cross Layer Analysis," *IEEE/ACM Trans. Networking,* vol. 17, no. 4, pp. 1186-1199, Aug. 2009.

[32] W. Ye, J. Heidemann, and D. Estrin, "Medium Access Control with Coordinated Adaptive Sleeping for Wireless Sensor Networks," *IEEE/ACM Trans. Networking,* vol. 12, no. 3, pp. 493-506, June 2004.

[33] M. Zuniga and B. Krishnamachari, "Analyzing the Transitional Region in Low Power Wireless Links," *Proc. IEEE Int'l Conf. Sensor and Ad Hoc Comm. and Networks (SECON '04),* pp. 517-526, Oct. 2004.

[34] TinyOS, http://www.tinyos.net, 2010.

Mehmet C. Vuran received the BSc degree in electrical and electronics engineering from Bilkent University, Ankara, Turkey, in 2002, and the MS and PhD degrees in electrical and computer engineering from the School of Electrical and Computer Engineering, Georgia Institute of Technology, Atlanta, in 2004 and 2007, respectively, under the supervision of Professor Ian F. Akyildiz. Currently, he is an assistant professor in the Department of Computer Science and Engineering at the University of Nebraska—Lincoln. His current research interests include cross-layer design, wireless sensor networks, underground sensor networks, cognitive radio networks, and deep space communication networks. He is a member of the IEEE and received the US National Science Foundation CAREER award in 2010.

Ian F. Akyildiz is the Ken Byers Chair Professor in the School of Electrical and Computer Engineering, director of the Broadband and Wireless Networking Laboratory, and chair of the Telecommunications Group at the Georgia Institute of Technology, Atlanta. He has been an honorary professor with the School of Electrical Engineering at the Universitat Politecnica de Catalunya and director of the NaNoNetworking Center (N3Cat) in Catalunya, Barcelona, Spain, since June 2008. He has been the editor-in-chief of *Computer Networks* (Elsevier) since 2000, and was the founding editor-in-chief of the *Ad Hoc Networks* journal (Elsevier) in 2003, the founding editor-in-chief of the *Physical Communication* (PHYCOM) journal (Elsevier) in 2008, and the founding editor-in-chief of the *Nano Communication Networks* (NANOCOMNET) journal (Elsevier) in 2010. He received the 1997 IEEE Leonard G. Abraham Prize Award (from the IEEE Communications Society), the 2003 IEEE Best Tutorial Award (from the IEEE Communications Society), and the Best Paper Award from the Ad Hoc and Sensor Networks (AHSN) Symposium at IEEE ICC in June 2009. He also received the 2002 IEEE Harry M. Goode Memorial Award (from the IEEE Computer Society) with the citation "for significant and pioneering contributions to advanced architectures and protocols for wireless and satellite networking" and the 2003 ACM SIGMOBILE Outstanding Contribution Award for "pioneering contributions in the area of mobility and resource management for wireless communication networks." Dr. Akyildiz is the author of two advanced textbooks, *Wireless Sensor Networks* and *Wireless Mesh Networks*, both published by John Wiley and Sons in August 2010 and February 2009, respectively. His current research interests are in wireless sensor networks, nanonetworks, and cognitive radio networks. He has been a fellow of the IEEE since 1996 and a fellow of the ACM since 1997.